Progress in X-ray plasma diagnostics

Jelle S. Kaastra[1,2], Ton Raassen[1,3], Cor de Vries[1]

[1] SRON Netherlands Institute for Space Research, Sorbonnelaan 2, 3584 CA Utrecht, the Netherlands
[2] Sterrenkundig Instituut, Universiteit Utrecht, P.O. Box 80000, 3508 TA Utrecht, The Netherlands
[3] Astronomical Institute "Anton Pannekoek", Kruislaan 403, 1098 SJ Amsterdam, The Netherlands
E-mail (JSK): j.s.kaastra@sron.nl

ABSTRACT

We discuss some interesting recent developments in X-ray plasma diagnostics. In collisionally ionised plasmas like clusters of galaxies, we show how various multi-temperature analysis techniques can be used in order to obtain the proper emission measure distribution and chemical abundances. We show how spectra from sources with non-thermal electron distributions can be modelled simply. We also discuss advances in the modelling of atomic processes that contribute to the final X-ray spectrum. Finally, we discuss progress in the modelling of X-ray absorption spectra.

KEY WORDS: Atomic data — Radiation mechanisms: general — X-rays: general

1. Introduction

Most spectroscopic codes started in the late 60's of the past century. For a historical overview of plasma models we refer to Raymond (2005). In this contribution we focus on the spectroscopic work in Utrecht, started in 1972 by Rolf Mewe. The original code evolved gradually over the years (see Raymond (2009) for a review of Mewe's most cited paper). The original spectroscopic models were integrated in a broader spectral fitting and analysis program, named SPEX, which originated in its earliest form in 1992 (see Kaastra et al. 1996b).

SPEX (www.sron.nl/spex) allows the user to calculate, display and fit spectra. It contains in particular thermal models under a broad range of physical conditions (CIE, NEI, PIE, etc.). It used the same atomic database for all of its models. The core of that is formed by the old Mewe et al. models (Mewe et al. 1985, 1986). However, several updates have been made, and extensive updates are in progress.

We want to stress here that under "normal" operating conditions, the older models work well. However, inspired by new data or data from new instruments, or new applications, the limitations of the models are sometimes surpassed. Our updates are often inspired by such new opportunities. In most cases, updating is a straightforward but time-consuming task, in particular the quality and completeness checks of code and data, and the benchmarking against other calculations. The old adagium "everyone wants to use it, nobody wants to do it" also applies here.

2. Updates of SPEX

As mentioned above, we are in the process of updating the atomic database that is being used for SPEX. Updates of collisional excitation rates are now completed for the most important iso-electronic sequences. These updates were obtained using calculations with different atomic codes such as HULLAC and FAC, or obtained from the literature. As an example, O VII had 7 lines available in the updated *mekal* code (based on Mewe et al. 1985), while the new version of SPEX has 2645 lines(up to $n = 20$ and including infrared transitions).

In addition, we extend our calculations from the 15 most abundant elements to all elements with nuclear charge $Z \leq 30$ (H to Zn).

For the calculation of a realistic spectrum, not only collisional excitation is important, but also other process typically contribute $\sim 10\%$ to the line flux under collisional ionisation (CIE) conditions, or even more under other circumstances. Currently we are updating the radiative recombination rates; other rates that need to be updated are the dielectronic recombination rates and inner-shell ionisation and excitation processes. Also, recently updates on the ionisation and recombination rates needed for the ionisation balance have become available, and these will also be included in the new version.

The updates of SPEX are not only restricted to atomic data. Recently, we have introduced a procedure to take account of non-Maxwellian electron distributions in the calculation of the X-ray spectra. This is described in detail by Kaastra et al. (2009b). It is in particular of potential interest for future high-resolution spectroscopic missions such as Astro-H or IXO. This is because in par-

ticular some satellite lines are sensitive to the presence of high-energy electrons, and only with high spectral resolution these weak lines can be disentangled from the stronger emission lines. SPEX now by default can handle these cases.

3. Multi-temperature plasmas

Another topic where we have been working on recently is the modelling of multi-temperature plasmas. In general, line emissivities are a smooth function of temperature. When multiple temperature components are present in the source, all these components can contribute to the flux of a single line. In order to derive the differential emission measure (DEM) distribution in the source, one therefore needs at least as many spectral lines as there are temperature components. But that is yet an insufficient condition. Because spectra from plasmas with temperatures that differ not too much are very similar, in practice it is hard to derive the precise shape of the DEM. At best, one may be able to derive the *total emission measure* and *average temperature* of the source over temperature ranges spanning typically a factor of 1.5–2. This is a well known problem, but not always recognised by those who analyse spectra. As long as the average temperature and total emission measure are the same over such a range, in practice the spectra are indistinguishable.

There are different solutions to this problem. An old solution is to do a DEM analysis on a grid of temperatures, and using different constraints such as regularisation or parameterisation of the DEM. An overview of such methods, as far as implemented in SPEX, was given by Kaastra et al. (1996a).

Originally triggered by the cooling flow problem for clusters of galaxies, we have also implemented parameterised forms of the DEM into SPEX. Two classes of models have proven to be rather successful in the analysis of clusters of galaxies.

The first model, called *wdem* in SPEX, parameterises the DEM with a power-law in temperature, DEM $\sim T^{1\alpha}$ up to a maximum temperature $T_{\max}$. In the limit of $\alpha \to 0$, this smoothly coincides with an isothermal mode. For non-zero α, it describes rather well the low-temperature tail in cool-core clusters.

The second model, often called *gdem*, adopts a DEM with a Gaussian distribution with width σ around the central temperature. Again, for $\sigma \to 0$ this coincides with an isothermal model. This model is in particular usefull for the outer parts of clusters; the extracted spectrum may be a combination of spectra from regions with differing temperatures.

Both models can be used to test how good an isothermal model applies to the data. In many cases, we have been able to show that significant deviations from isothermality occurs. All this is not only of relevance to derive the proper DEM distribution of the source, but it also may affect the derived abundances. This is because the line emissivity, a good abundance diagnostic, is temperature dependent. We only mention here an example from the work of De Plaa et al. (2006) for the inner 4 arcmin core of the cluster Sérsic 159−3. Changing from isothermal to *wdem* to *gdem*, χ^2 decreased from 1228 to 1217 to 949, for 916–914 degrees of freedom. At the same time, the iron abundance changed significantly from 0.36 to 0.35 to 0.24, and oxygen from 0.36 to 0.30 and 0.19. Thus, for deriving accurate and unbiased abundances in clusters of galaxies, stellar coronae or any other source with thermal X-ray emission, it is very important to reconstruct accurately the temperature distribution, and the *wdem* and *gdem* models are useful tools for that.

4. Spatially extended sources with RGS

The Reflection Grating Spectrometer (RGS) of XMM-Newton disperses the light of extended sources in one particular direction on the sky image of the source. Therefore, the observed spectra of extended sources contain the spatial and spectral information in a coupled way. The same also holds for the grating spectrometers on Chandra. Fortunately, there is a linear relation between the off-axis angle of the photon source and the wavelength shift of the photons in the dispersed spectrum. SPEX contains a convolution model, where this effect can be taken into account during spectral fitting. One starts with an X-ray image of the source, preferentially in the same energy band as RGS, and collapses that onto the dispersion axis of RGS (taking account of the finite width of the RGS in the cross-dispersion direction). This one-dimensional image then serves as a convolution kernel, with which the model spectrum is convolved before folding with the response matrix.

A basic assumption is here that the spectrum at each position in the source is the same. In practice, this is not always the case, but it is a good first approximation. SPEX allows the width to be varied during the fitting process, and it is sometimes possible to separate two different spectral components. For instance, we have succesfully used different widths for the oxygen and iron lines in the RGS spectra of clusters of galaxies (e.g. Werner et al. 2006).

A good example where these methods can be applied are also groups of galaxies. Recently, Werner et al. (2009) used these techniques to demonstrate the lack of resonance scattering in some of these groups and to place an upper limit to the amount of turbulence.

5. Interstellar absorption cross sections

For most X-ray astronomers, interstellar absorption is a nuisance, in the sense that it eats away valuable X-ray

photons that otherwise could have been used to determine the properties of the studied X-ray sources. However, the imprint of the absorption offers valuable information on the interstellar medium itself. In particular the advent of X-ray grating spectrometers has made such studies possible.

These high-resolution observations show that the absorption edges of the most important elements are not simply infinitely sharp structures. They show a lot of structure, both due to the fact that often more quantum states are possible, and due to resonances that can already cause absorption at energies below the ionisation potential of the relevant atomic level. Moreover, close to these edges the high-resolution spectra show the presence of discrete resonance absorption lines.

5.1.   Oxygen edge

One of the most important astrophysical edges is the oxygen edge. Theoretical calculations (e.g. McLaughlin & Kirby 1998) show a wealth of structure in the edge, but have difficulty to precisely predict the energies of these structures (at least with the accuracy that we now can observe with gratings from space). Ideally, laboratory experiments can provide the precise position of these resonances. For oxygen, this has been a major problem, however, due to contradictory results from different groups that we discuss below. There has been even more confusion due to the fact that in the interstellar medium about half of all oxygen atoms are bound in molecules or dust. Due to the molecular interactions, the edge structure changes significantly. This offers of course a unique opportunity to study dust through X-ray absorption, as each molecule has its own characteristic absorption structure. However, not all relevant cross-section are sufficiently well known. In addition, due to limited spectral resolution of the X-ray spectrometers, or sometimes due to limited statistics of the spectra, edges may be seen blurred and blended with the discrete resonance structures. This has led some authors to define "the" edge as the energy where in the observed spectrum the flux drops rapidly. However, here we prefer to retain the definition of the edge as the series limit of discrete absorption lines.

5.1.1.   Laboratory measurements

We now turn to the laboratory data for *atomic* oxygen. In Fig. 1 we show the difference between the measured energies of resonances for two sets of measurements, those of Menzel et al. (1996) and Stolte et al. (1997). A few things can be seen from this plot. First, there is a systematic, almost linear change of the energy differences with energy. This may be attributed due to small remaining calibration uncertainties in at least one of the two datasets. Further, from the scatter around the correlation it is seen that the correlation between
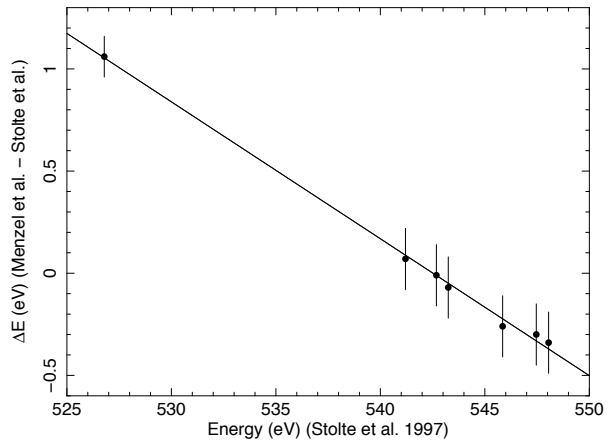
Fig. 1. Differences between the measured energies of resonances by Menzel et al. (1996) as compared to the measurements of Stolte et al. (1997).

both datasets is much better than suggested by the formal error bars. This is probably due to the fact that the error bars include a systematic uncertainty, that may be nearly the same for all transitions. From a linear regression we obtain for this energy difference (all units here in eV): $\Delta E = (36.357 \pm 0.010) - (0.0670 \pm 0.0016)E$, with a scatter of 0.03 eV (much smaller than the nominal uncertainties of 0.10 eV).

Next we compare the measurements of Krause (1994) and Caldwell et al. (1994) with those of Stolte et al. (1997). In this case, we find no significant slope (best fit 0.0029 ± 0.0037), and only a constant offset of 0.444 ± 0.028 eV. We conclude from this that apparently the relative energy scales of Krause (1994), Caldwell et al. (1994) and Stolte et al. (1997) agree, and that most likely the energy scale of Menzel et al. is slightly off. All these data sets, however, show a different offset for their absolute energy scale. We can resolve this by comparing to astrophysical measurements.

5.1.2.   The energy of the O I 1s-2p blend

.

We have measured the wavelength of the O I 1s-2p line using the well-exposed XMM-Newton RGS spectrum of Mrk 421 (Kaastra et al. 2006). This spectrum shows a strong interstellar 1s-2p absorption line, measured at 23.5138 ± 0.0022 Å. At the same CCD, also the 1s-2p resonance absorption line of O VII is present at 21.6027 ± 0.0021 Å. As the theoretical wavelength of this line is at 21.6019 Å, there is a small offset on the wavelength scale for this data set of 0.0008 mÅ, well within the systematic uncertainty of the RGS. Correcting for this small difference (and implicitly assuming that the O VII line shows no intrinsic redshift), we find an energy of 527.30 ± 0.05 eV for the O I 1s-2p line. Juett et al. (2004) also measured the 1s-2p line of O I using Chandra

HETGS spectra towards several compact X-ray binaries. Their value of 527.41 ± 0.07 eV is within the systematic uncertainty of the HETGS energy scale (± 0.24 eV) consistent with the value obtained with RGS. Taking the weighted average of both data sets, we obtain an energy of 527.34 ± 0.04 eV. Using this energy, we now can correct the energy scales of Stolte et al. (1997), Krause (1994) and Caldwell et al. (1994).

As a check, we have also measured the energy of the 1s-3p line of O I in the Mrk 421 RGS spectrum, and we have calculated the weighted mean of the values given by Juett et al. (2004). After correction, there is good agreement between the laboratory measurements and the astrophysical measurements, as we show in Table 1.

Table 1. Measured and corrected line energies (eV) of O I lines

Dataset	1s-2p	1s-3p
Astrophysical:		
Mrk 421	527.30 ± 0.05	541.95 ± 0.28
Juett et al. (2004)	527.41 ± 0.07	541.98 ± 0.19
weighted average:	527.34 ± 0.04	
Lab measurements:		
Stolte et al. (1997)	526.79 ± 0.04	541.20 ± 0.04
Krause (1994),		
Caldwell et al. (1994)	527.20 ± 0.30	
Menzel et al. (1996)	527.85 ± 0.10	541.27 ± 0.15
Lab measurements, corrected:		
Stolte et al. (1997)	527.34	541.75
Menzel et al. (1996)	527.85 ± 0.10	541.72

Using the same correction factor of $+0.55 \pm 0.06$ eV, we can correct the series limit of the ^4P and ^2P line series as derived by Stolte et al. (1997), and therefore find for these edge energies values of 544.58 and 549.40 eV, respectively. In our SPEX code, we have included the strongest absorption lines of O I, and have adjusted the calculated energies of the relevant lines according to the corrected measurements of Stolte et al. (1997).

The above calculations are valid for atomic oxygen. We have also introduced an absorption model for oxygen in bound form in SPEX, using cross sections collected from different sources. An example is shown in Fig. 13b of Kaastra et al. (2008).

5.2. Nitrogen edge

For the Nitrogen edge, there is similar confusion as for the oxygen edge. However, as nitrogen is almost purely atomic in the interstellar medium, the situation is somewhat simpler. The N I K-edge in SPEX was taken from the compilation of Lotz (1970), and corresponds to 30.77 Å. The only laboratory measurement available (Sant'Anna et al. 2000) shows two levels: the [^{3}D] limit

at 29.87 Å, and the [^{5}S] limit at 30.26 Å. This is off by 0.5–0.9 Å from the older value, and easily detected in grating spectra. In fact, the N I edge as measured in the Crab nebula (Kaastra et al. 2009) is in full agreement with these laboratory measurements. In addition, the measured energy of the 1s-2p line of N I in Sco X-1 fully agrees with the lab measurements of Sant'Anna et al. (De Vries et al. 2009, in preparation).

References

Caldwell, C.D., Schaphorst, S.J., Krause, M.O., & Jiménez-Mier, J. 1994 J.El.Spec.Relat.Phenom., 67, 243

de Plaa, J., Werner, N., Bykov, A.M. et al. 2006 A&A, 452, 397

Juett, A.M., Schulz, N.S. & Chakrabarty, D. 2004 ApJ, 612, 308

Kaastra, J.S., Mewe, R., Liedahl, D.A. et al. 1996a A&A, 314, 547

Kaastra, J.S., Mewe, R., & Nieuwenhuijzen, H. 1996b, Proc. 11th Coll. on UV and X-ray Spectroscopy of Astrophys. and Lab. Plasmas, p. 411

Kaastra, J.S., Werner, N., den Herder, J.W.A. et al. 2006 ApJ, 652, 189

Kaastra, J.S., Paerels, F.B.S., Durret, F., Schindler, S. & Richter, P. 2008 SSRv, 134, 155

Kaastra, J.S., de Vries, C.P., Costantini, E. & den Herder, J.W.A. 2009a A&A, 497, 291

Kaastra, J.S., Bykov, A.M.. & Werner, N. 2009b A&A, 503, 373

Krause, M.O. 1994 Nucl. Instrum. Methods B, 87, 182

Lotz, W. 1970 JOSA, 60, 206

McLaughlin, B.M., Kirby, K.P. 1998 JPhys B, 31, 4991

Menzel, A., Benzaid, S., Krause, M.O. et al. 1996 Phys Rev A, 54, R991

Mewe, R., Gronenschild, E.H.B.M. & van den Oord, G.H.J. 1985 A&AS, 62, 197

Mewe, R., Lemen, J.R. & van den Oord, G.H.J. 1986 A&AS, 65, 511

Raymond, J.C. 2005 AIP Conf. Proc., 774, 15

Raymond, J.C. 2009 A&A, 500, 311

Sant'Anna, M.M., Stolte, W.C., Öhrwall, G. et al. 2000, abstract, available at http:// www.als.lbl.gov/ als/ compendium/ AbstractManager/ uploads/00029.pdf

Stolte, W.C., Lu, Y., Samson, J.A.R. et al. 1997 J Phys B, 30, 4489

Werner, N., de Plaa, J., Kaastra, J.S. et al. 2006 A&A, 449, 475

Werner, N. et al. 2009 MNRAS, 398, 23